# We are IntechOpen, the world's leading publisher of Open Access books
# Built by scientists, for scientists

**4,800**
Open access books available

**122,000**
International authors and editors

**135M**
Downloads

Our authors are among the

**154**
Countries delivered to

**TOP 1%**
most cited scientists

**12.2%**
Contributors from top 500 universities

CLARIVATE ANALYTICS
BOOK CITATION INDEX
INDEXED

WEB OF SCIENCE™

Selection of our books indexed in the Book Citation Index in Web of Science™ Core Collection (BKCI)

## Interested in publishing with us?
## Contact book.department@intechopen.com

Numbers displayed above are based on latest data collected.
For more information visit www.intechopen.com

Chapter 12

# Cable Effects on Measuring Small Planar UWB Monopole Antennas

L. Liu, S.W. Cheung, Y.F. Weng and T.I. Yuk

Additional information is available at the end of the chapter

http://dx.doi.org/10.5772/46080

## 1. Introduction

Since the US-FCC assigned the ultrawide band (UWB) for unlicensed use in 2002, UWB technology has attracted much attention in both the commercial and academic domains. The characteristics of ultrawide bandwidth from 3.1 to 10.6 GHz and low power emission of -41.3 dBm/MHz make it a promising candidate for different applications such as high speed communications and radar imaging systems. However, the requirements for impedance matching, constant gain, constant radiation patterns and high radiation efficiency over such a wide bandwidth for the UWB antenna become great challenges to antenna designers.

With the increasing demand for smaller wireless devices, planar antenna, with the advantages of compact size, low profile, low cost, ease of fabrication and ease of integration with RF circuits, appears to be more preferable for UWB applications. Among different planar antennas, monopole antenna has the simplest structure, compact size and omnidirectional radiation pattern and so is one of the best candidates. For a planar monopole antenna to work properly, the ground plane is required to be electrically large enough to approximate an infinite-ground plane and so occupies a large portion of the overall antenna size. Thus to design a compact UWB monopole antenna, the ground plane is usually the one to be minimized. Designing a planar monopole antenna with a small ground plane to cover the UWB is not a difficult task and can be achieved through different techniques [1-7]. The design is usually done using computer simulation. In carrying out the design in simulation, the antenna is fed directly with a signal source without using a feeding cable. However, when the final design is completed and prototyped for measurements, a feeding cable is normally used to connect the antenna to the measurement system. The small ground plane cannot approximate an infinite ground plane well and causes the currents to flow back to the outer surface of the feeding cable, resulting in secondary radiation. This leads to discrepancies between the simulated and measured performances of the antenna and creates uncertainties to the design of the antenna.

INTECH
open science | open minds

© 2012 Liu et al., licensee InTech. This is an open access chapter distributed under the terms of the Creative Commons Attribution License (http://creativecommons.org/licenses/by/3.0), which permits unrestricted use, distribution, and reproduction in any medium, provided the original work is properly cited.

To resolve the problem, a sleeve balun can be placed at the end of the cable to prevent currents from flowing back to the feeding cable [8,9]. A sleeve balun is a metal tube with a length of quarter-wavelength to provide an open circuit for the signal. Although sleeve baluns can be designed to possess good choking characteristics, they are narrowband devices and so are not suitable for UWB antennas. For wideband and high-frequency operation, the feeding cable can be covered with an EMI suppressant material to absorb unwanted EM radiation [10]. By using this method, the shape of the measured and simulated radiation patterns of the antenna will be similar, but the measured efficiency and gain will be lower due to the energy absorbed by the EMI suppressant material. The discrepancies again produce uncertainties to the design of the antenna.

In this chapter, the effects of ground-plane size and feeding cable on the measurements of small UWB monopole antennas are investigated. A group of nine planar UWB monopoles with an identical elliptical radiators but different ground-plane sizes are designed using computer simulation where no feeding cable is used. These antennas are also prototyped and measured using the antenna measurement system, Satimo Starlab, where a feeding cable is used [11]. The simulated and measured performances show large discrepancies at low frequencies. To investigate the discrepancies, two different types of feeding cables, a high-frequency coaxial cable and a high-frequency coaxial cable with EMI suppressant tubing, are studied. The simulation models for the two cables are developed and used in computer simulation. With the application of the two cable models, the simulated and measured performances show good agreements. The results show that the feeding cable without EMI suppressant tubing causes many ripples on the 3D-radiation patterns of the antenna.

## 2. UWB monopole antennas

Dipole antenna, often called dipole, is one of the simplest but most widely used types of antennas. The typical structure of a dipole consists of two thin-wire conductors normally having equal length $L$ as shown in Figure 1(a) where it is assumed $L=\lambda/2$ with $\lambda$ being the wavelength at the resonant frequency. At resonance, the currents form the standing waves on both conductors, as shown in Figure 1(a), giving rise to electromagnetic (EM) radiations. Monopole antenna, often called monopole, has half the size of a dipole. An ideal monopole normally consists of a single thin-wire conductor perpendicularly mounted on an infinite ground plane as shown in Figure 1(b). At resonance, the current forms a standing wave on the conductor which radiates EM fields. The EM fields incident on the infinite ground plane are reflected as if they were radiated from the monopole image having the same current distribution as that of the lower conductor of the dipole in Figure 1(a). Thus a monopole can be viewed as the corresponding double-length center-fed linear dipole [12]. A monopole radiates energy into only the upper half space. So for a given input power, a monopole has the radiated power and hence the gain twice as much as the corresponding dipole.

A thin-wire monopole has a simple structure, but a very narrow bandwidth, making it unsuitable for UWB applications. To broaden the impedance bandwidth, the thin-wire

conductor can be made flat to become a planar element and then laid parallel to the ground plane to form a low-profile planar monopole. The planar element can take on different shapes as shown in Figure 2 [13].

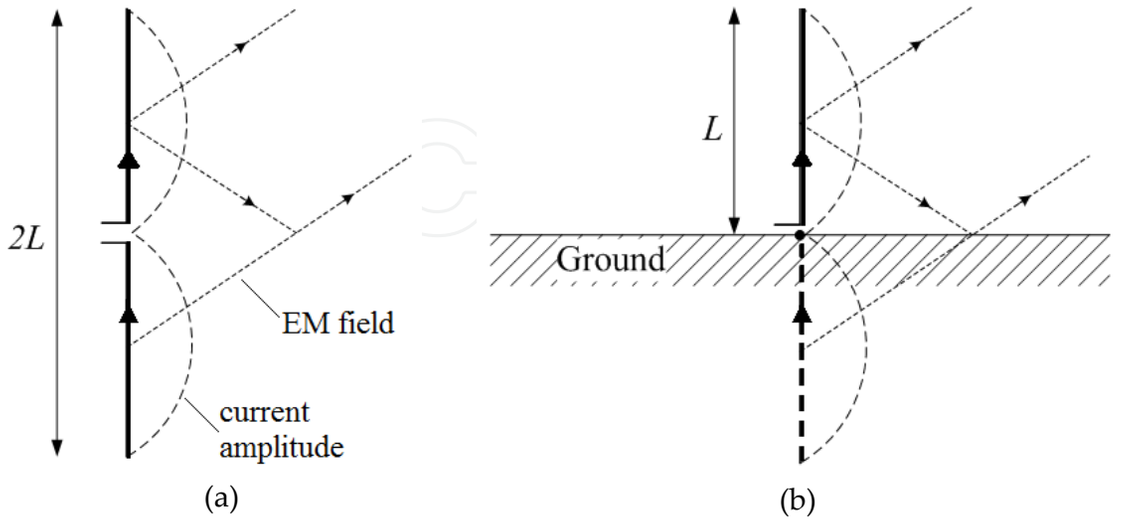


**Figure 1.** (a) Center-fed dipole and (b) vertical monopole above infinite ground

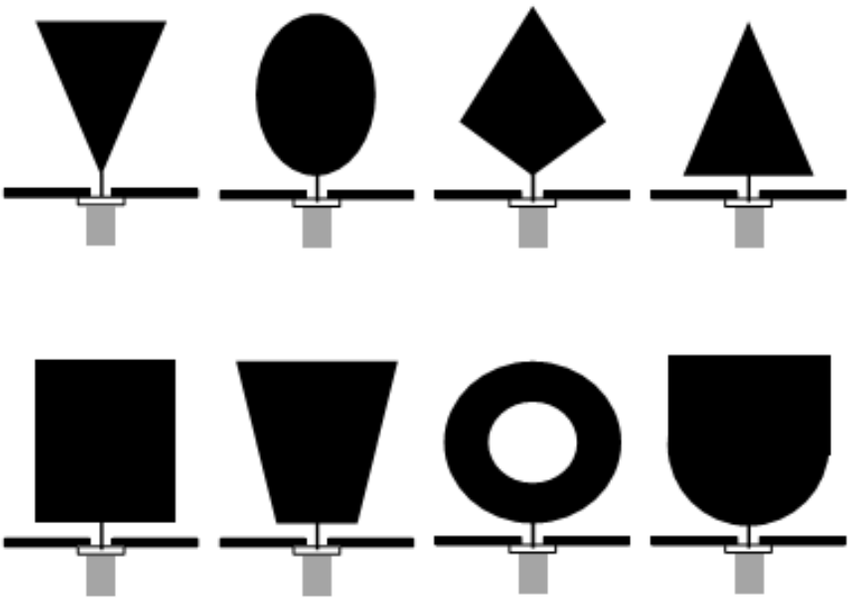

**Figure 2.** Planar monopoles using different radiator shapes [13]

## 3. Effects of ground plane on small UWB monopoles measurements

With the increasing demand for smaller wireless devices, planar monopole antennas with small ground planes have attract much attention. However, in the design of such an antenna, very often, after the antenna performance in terms of gain, efficiency and return

loss has been optimized using computer simulation, the measured performance of the prototyped antenna does not agree with the simulated performance. Large discrepancies usually occur at lower frequencies. This creates uncertainties and doubts in the design of the antenna. As will be shown in the following sections, the discrepancies at low frequencies are mainly caused by the feeding cable used to connect the antenna to the measurement system.

### 3.1. Cable effects on measuring monopoles with small ground planes

Nowadays, the design of antennas is usually done by using computer simulation. In simulation, normally the antenna is directly fed from a signal source and no feeding cable is used. However, when the antenna is fabricated and measured in a practical situation, a feeding cable is always used to connect the antenna to the measurement system and the signal is fed through the feeding cable to the antenna. In such arrangement, the cable could affect the measured results in two possible ways [14] as illustrated in Figure 3.

Since the feeding cable is quite near to the radiator and so is in the near field region of the antenna, the radiated EM fields incident on the cable will be scattered and reflected as shown in Figure 3(a). The feeding cable becomes a parasitic element [15]. Due to the small size of the cable, this cable effect on the measurement results is relatively small.

If the antenna is a planar monopole with a small ground plane, some EM fields will not be reflected as in the case of having an infinite ground plane shown in Figure 1(b). Instead, the EM fields arriving at the edges of the small ground plane will be diffracted. This induces surface currents to flow back on the outer surface of the feeding cable, resulting in secondary radiation as shown in Figure 3(b). This effect on measurements could be quite significant, depending on the electrical size of the ground plane. Computer simulation is carried out to study the effects of using large and small ground planes of a thin-wire monopole antenna fed by a coaxial cable on the Electric fields (E-fields). The large and small ground planes have a circular shape with the radii of $2.06\lambda$ and $0.41\lambda$, respectively, and a thickness of $0.0008\lambda$, where $\lambda$ is the wavelength at the resonant frequency. The length of feeding cable is $1.64\lambda$. Figure 4(a) shows a snap-shot of the E-fields radiated from the monopole antenna using the small ground plane. It can be seen that the E-fields arriving at the edges of the ground plane are quite strong. The ground-plane edges diffract the strong incident E-fields in all directions [16, 17]. After diffraction, some of the E-fields go to the upper free space and others go to the lower free space with respect to the ground plane. A significant portion of the E-fields diffracts onto the bottom surface of the ground plane, which will induce surface currents. The surface currents will flow towards the feeding cable at the center of the ground plane and onto the outer conductor-surface of the cable. Figure 4(a) shows that a standing wave is formed on the feeding cable and this will result in "secondary radiation" and affect the measured results. When the large ground plane with a radius of $2.06\lambda$ is used, Figure 4(b) shows a snap-shot of the E-fields radiating from the monopole antenna. It can be seen that the E-fields arriving at the edge of the ground plane are quite weak. As a result, the induced currents on the bottom surface of the ground plane and hence the currents flowing back onto the outer conductor-surface of the feeding cable are very weak. In this case, secondary radiation is much less.

The simulated 3D-radiation patterns for the two cases are shown in Figures 4(c) and (d). It can be seen that both radiation patterns have peak-radiation at elevation from the horizontal ground plane, typical for monopoles with finite ground planes. For the antenna with the large ground, peak-radiation is stronger and at a smaller elevation angle than those for the antenna with the small ground plane. Peak-radiation in the lower hemisphere of the radiation pattern is much weaker for the antenna with the large ground than for the antenna with the small ground plane. For the antenna with the small ground plane, Figure 4(c) shows that ripples occur in both the upper and lower hemispheres of the pattern. However, for the antenna with the large ground plane, Figures 4(d) shows no ripple in the upper hemisphere of the pattern, but many ripples with much smaller magnitudes in the lower hemisphere.

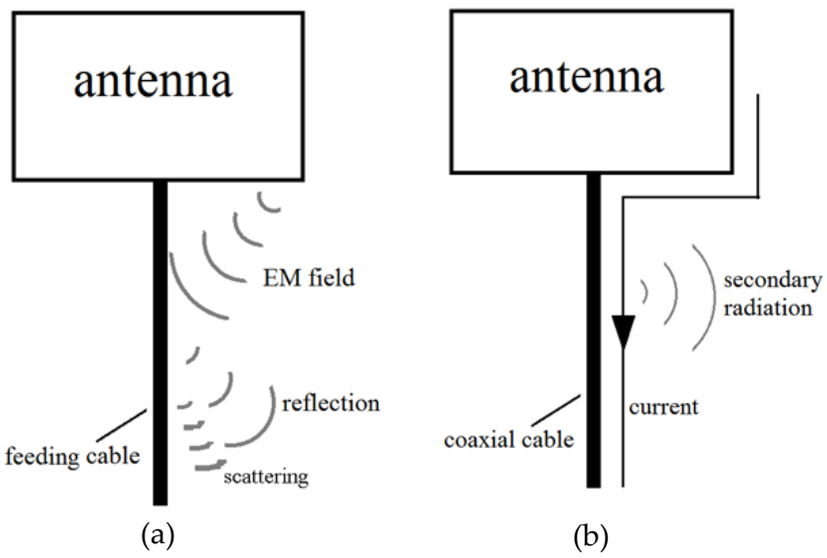


**Figure 3.** Illustration of two possible ways affecting measured results of antenna: (a) reflections of EM fields from antenna and (b) currents flowing back to feeding cable

Ripples on a 3D-radiation pattern are the results of EM fields with different phases adding together constructively and destructively in different spatial directions. To study the causes of these ripples on the 3D-radiation patterns of Figures 4(c) and (d), computer simulation is carried out on the same antenna with the same large and small ground planes but without using the feeding cable. Results at resonant frequency are shown in Figure 5. For the antenna with the small ground plane, Figure 5(a) shows that the ripples disappear. Thus the ripples in Figure 4(c) are mainly caused by the feeding cable. In fact, this agrees with Figure 4(a) which shows that, at the resonant frequency, a standing wave is developed on the feeding cable which gives out EM radiation. The EM fields are added together constructively and destructively in different spatial directions, producing ripples in the 3D-radiation pattern in Figure 4(c). For the antenna with the large ground plane and without using the feeding cable, Figure 5(b) shows that the 3D-radiation pattern is about the same as that in Figure 4(d) using the feeding cable. This agrees with Figure 4(b) which shows no standing wave developed on the feeding cable and so no radiation from the cable. Thus the feeding cable has no effect on the radiation pattern. However, Figure 5(b) shows that the

ripples still occur in the lower hemisphere of the pattern. This indicates that the ripples are mainly caused by diffraction of EM fields at the edges of the ground plane. The reason can be explained as follows. The EM fields radiated from the monopole are diffracted at the edge of the ground plane into free space below the ground plane. Since the ground plane has a diameter of $4.12\lambda$, the diffracted EM fields are added together constructively and destructively in different spatial directions in the lower hemisphere, forming many ripples in the radiation pattern.

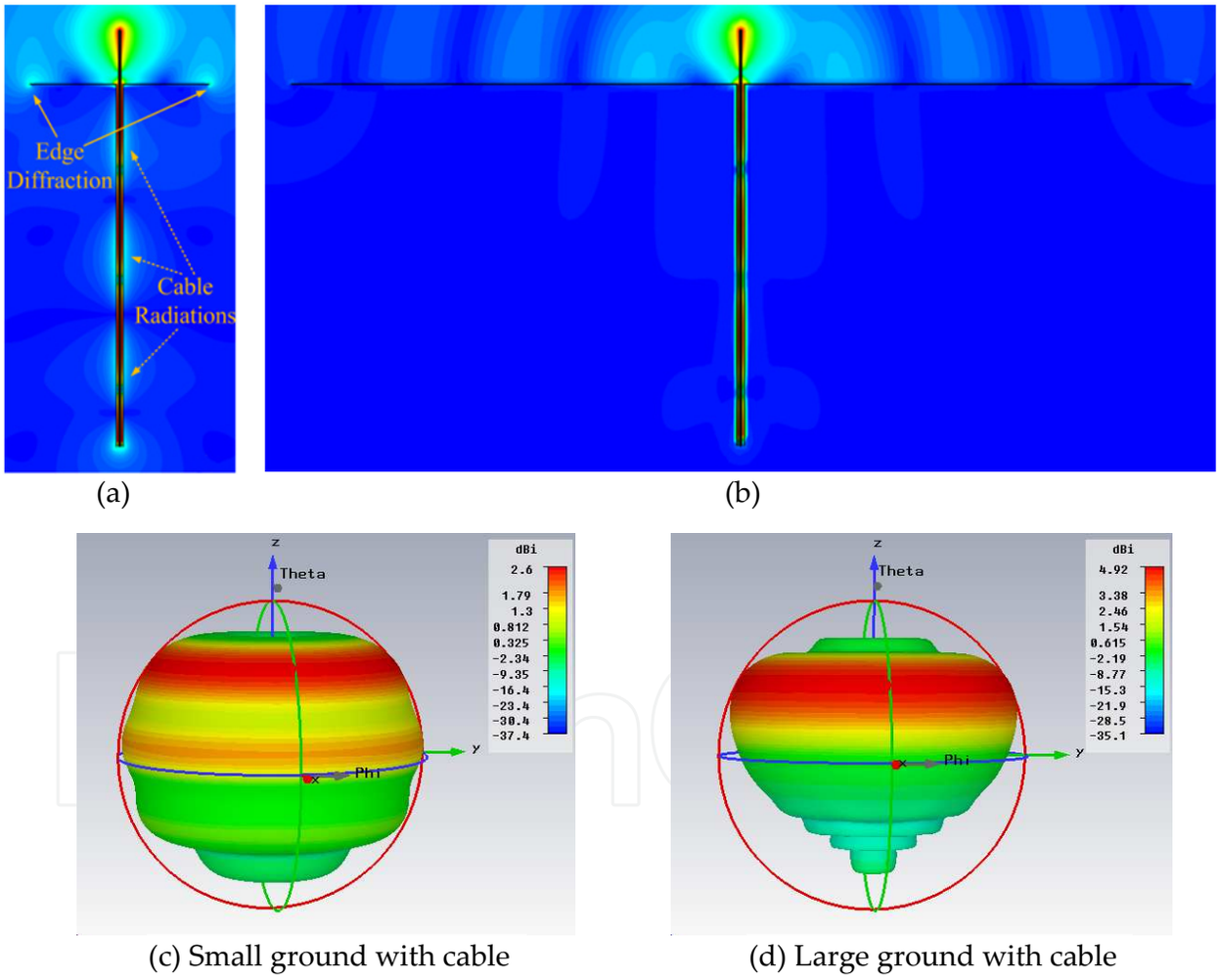


**Figure 4.** E-field radiation of thin-wire monopole antenna fed using coaxial cable for (a) small ground plane and (b) large ground plane, and corresponding radiation patterns (c) and (d).

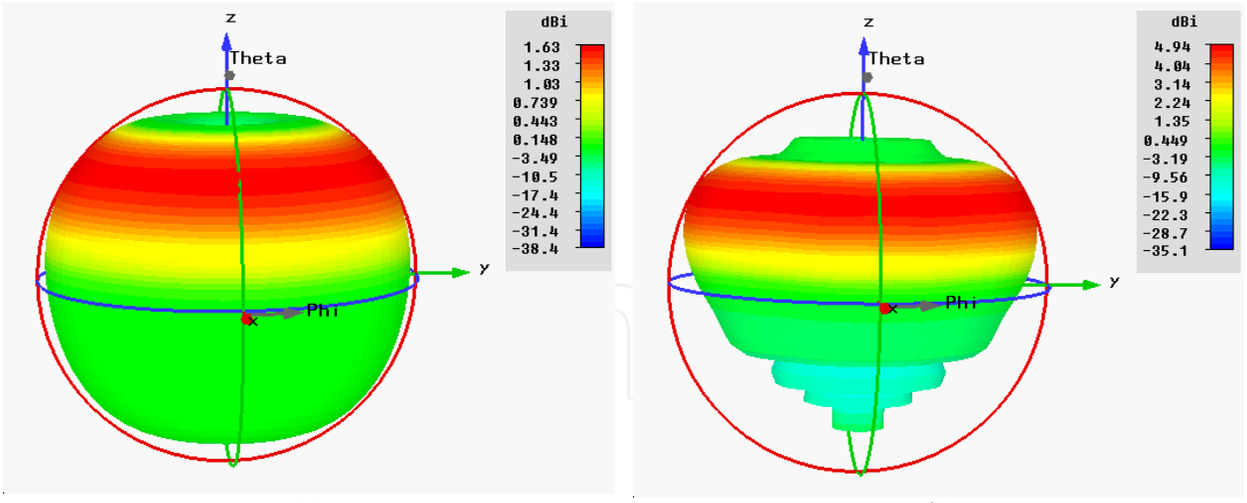


**Figure 5.** Radiation patterns of thin-wire monopole antenna without using feeding cable (a) small ground plane, and (b) large ground plane

## 3.2. Studies of UWB monopole antennas with different ground-plane sizes

### *3.2.1. Structure of the antennas*

To investigate the effects of ground-plane size on measurements of small UWB monopole antennas, a group of nine antennas, Ants 1, 2, …, 9, are used. These antennas have an identical elliptical-shaped radiator printed on one side of the substrate but a ground plane with different sizes on the other side of the substrate [18]. They are designed on the Rogers substrate, RO4350, with a relative dielectric constant of 3.48, a thickness of 0.762 mm and a loss tangent of 0.0037, as shown in Figure 6.

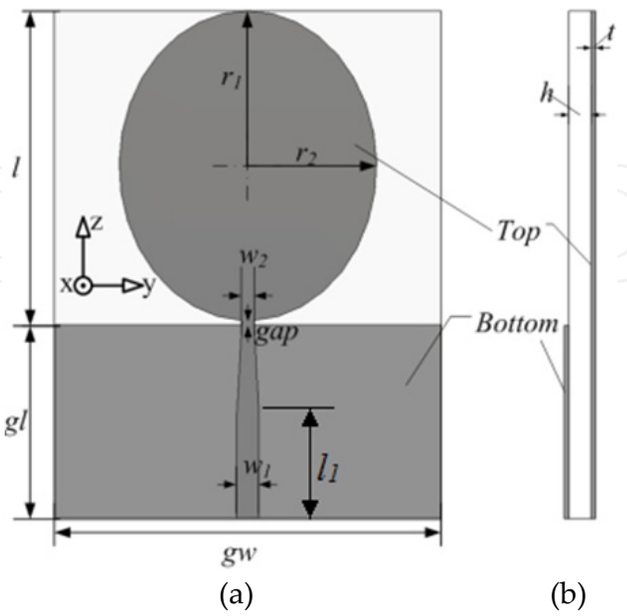


**Figure 6.** Structure of UWB antennas: (a) top view and (b) side view

The tapered microstrip feed line and the gap between the radiator and the ground plane are important factors for impedance matching and so are optimized for maximum impedance bandwidth using computer simulation. The optimized dimensions of these nine antennas are listed in Table 1.

| *Antenna* | *gl×gw* | $w_1$ | $w_2$ | $l_1$ | *gap* | $r_1$ | $r_2$ | *Antenna* | *gl×gw* | $w_1$ | $w_2$ | $l_1$ | *gap* | $r_1$ | $r_2$ |
|---|---|---|---|---|---|---|---|---|---|---|---|---|---|---|---|
| ***Ant 1*** | *15×30* | *1.73* | *0.9* | *8* | *0.3* | *12* | *11* | ***Ant 6*** | *30×80* | *1.73* | *0.83* | *23* | *0.3* | *12* | *11* |
| ***Ant 2*** | *15×50* | *1.73* | *0.76* | *5* | *0.2* | *12* | *11* | ***Ant 7*** | *50×30* | *1.73* | *0.94* | *44* | *0.3* | *12* | *11* |
| ***Ant 3*** | *15×80* | *1.73* | *0.72* | *3* | *0.3* | *12* | *11* | ***Ant 8*** | *50×50* | *1.73* | *0.69* | *43* | *0.3* | *12* | *11* |
| ***Ant 4*** | *30×30* | *1.73* | *0.9* | *23* | *0.3* | *12* | *11* | ***Ant 9*** | *50×80* | *1.73* | *0.72* | *38* | *0.3* | *12* | *11* |
| ***Ant 5*** | *30×50* | *1.73* | *0.83* | *23* | *0.3* | *12* | *11* | | | | | | | | |

**Table 1.** Ground-plane dimensions of antennas (unit: mm)

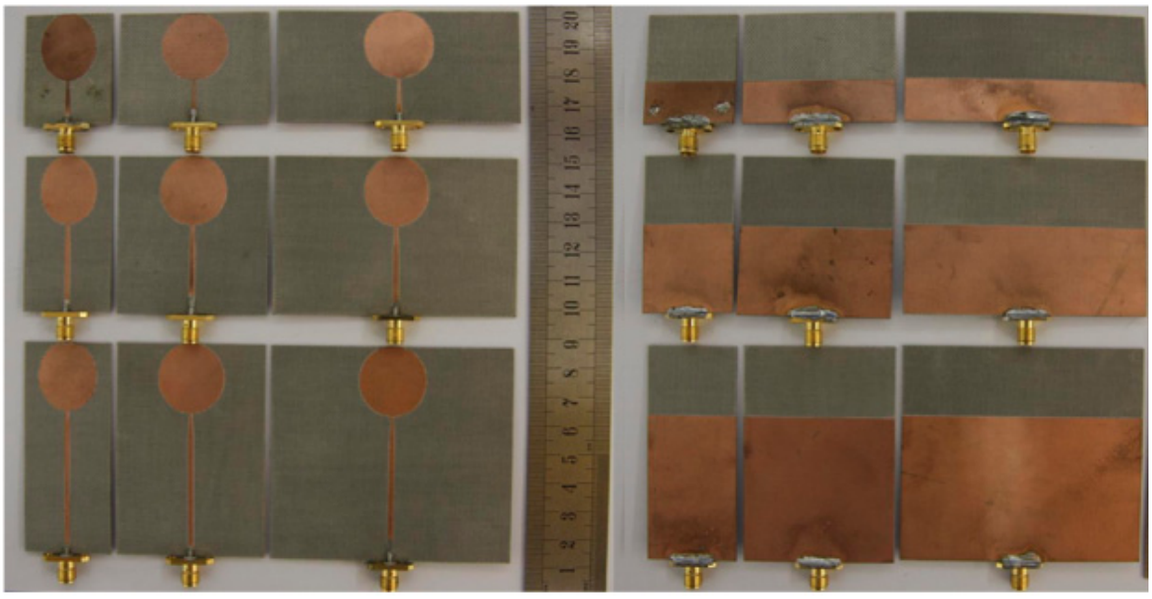

(a) (b)

**Figure 7.** Prototypes of nine planar monopole antennas with different ground-plane sizes: (a) top view and (b) bottom view.

### *3.2.2. Results and discussions*

The performances of the nine antennas, in terms of $S_{11}$ and efficiency, are studied by computer simulation. In simulation, no feeding cable is used and the antennas are fed directly by the signal source. Using the optimized dimensions in Table 1, the nine antennas are also prototyped using the Rogers substrate, RO4350, as shown in Figure 7, and measured using the antenna measurement system, Satimo Starlab, shown in Figure 8. In measurements, of course, a feeding cable with an SMA connector (provided by Satimo) is used to connect the antennas to the Starlab system. The cable is enclosed by an EMI suppressant tube to absorb EM radiation. The simulated and measured $S_{11}$ and efficiencies of the antennas are shown in Figure 9. It can be seen that the simulated and measured impedance bandwidths ($S_{11}$<-10 dB) for all antennas show good agreements. However, for

efficiency, the measured results are always lower than the simulated results. The discrepancies are more obvious for antennas with smaller ground planes and at lower frequencies.

To examine the effects of ground-plane size on the discrepancy of efficiency, we divide the whole frequency band from 2 to 12 GHz into three sub-bands, i.e. 2-4 GHz, 4-6 GHz, and 6-12 GHz, and compute the average discrepancy in the whole band and in each of the sub-bands. Results are listed in Table 2, where each row has the same ground-plane width and increasing length and each column has the same ground-plane length and increasing width. From Figure 9 and Table 2, we can observe the following phenomena:

1. The lower cut-off frequency reduces with increasing ground-plane length (gl).

In Figures 9(a), (b) and (c), the ground planes have the same length of 15 mm but different widths. The lower cut-off frequencies ($S_{11}$=-10 dB) of the antennas are all at about 2.8 GHz. This phenomenon is also observed in Figures 9(d), (e) and (f), and in Figures 9(g), (h) and (i).

In Figures 9(a), (d) and (g), the ground planes have the same width. As the ground-plane length increases from 15 to 30 and 50 mm, the lower cut-off frequency decreases from 2.76 to 2.38 to 2.21, respectively. This phenomenon is also observed in Figures 9(b), (e) and (h), and Figures 9(c), (f) and (i). Thus the lower cut-off frequency reduces with increasing ground-plane length (*gl*).

For dipole antenna, the lower cut-off frequency is inversely proportional to the length of the radiator. The results in Figure 9 show that the monopole antennas with small ground planes behave like asymmetric dipole antennas [19] and the lower cut-off frequency is inversely proportional to the length of the ground plane.

2. Discrepancy reduces with increasing frequency

Figure 9 shows that the discrepancy is larger at lower frequencies and smaller at higher frequencies. This phenomenon can also be observed in Table 2 which shows the discrepancy is always smallest in the higher sub-band and largest in the lower sub-band. This is because at higher frequencies, the ground plane becomes electrically larger.

3. Discrepancy reduces with increasing ground-plane width and ground-plane length.

Table 2 shows the discrepancy reduces with increasing ground-plane width and ground-plane length.

4. The width of ground plane has more effect on the efficiency than the length.

Each row in Table 2 represents the ground planes of the same widths but different lengths. Table 2 shows the average discrepancy through 2-12 GHz decreases significantly with increasing ground-plane length. Each column in Table 2 represents the ground planes of the same length but different widths and the results show the discrepancy does not change much. This can also be seen in Figure 9 by comparing the simulated and measured efficiencies of the corresponding antennas. These results show that increasing the ground-plane width has more effect on reducing the discrepancy than increasing the ground-plane

length. This is because a small ground plane serves as a radiator and the width of the radiator improves the impedance bandwidth.

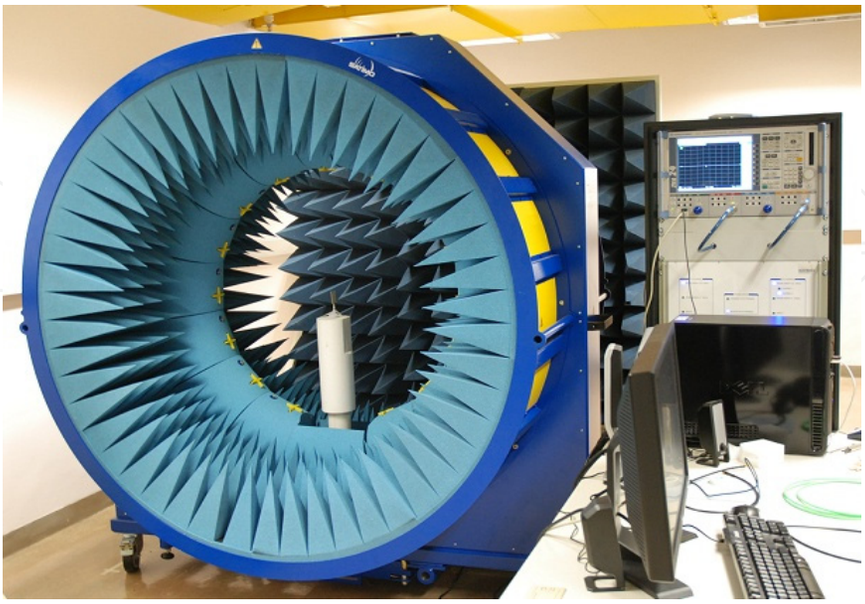

**Figure 8.** Antenna in Starlab system for measurement

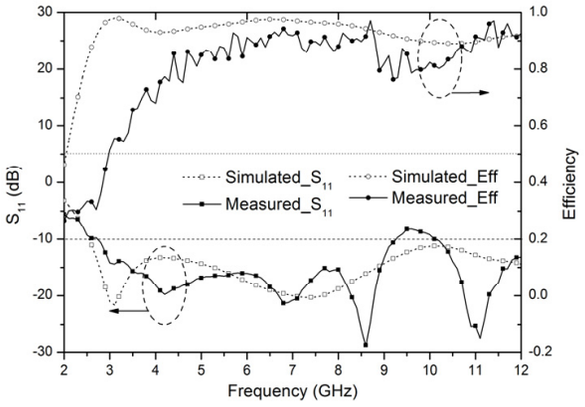


(a) Ant 1: 15×30 mm²

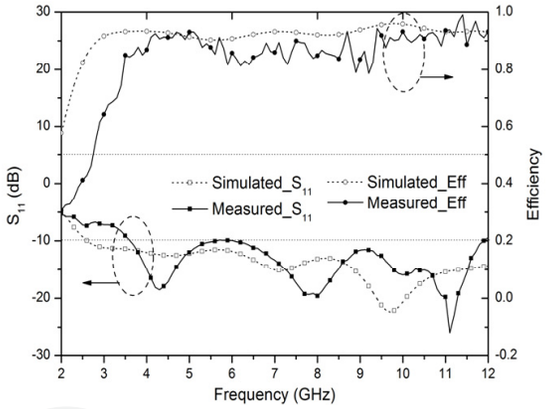


(b) Ant 2: 15×50 mm²

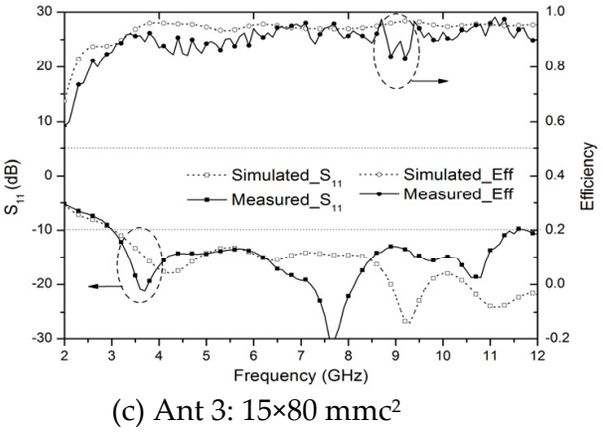


(c) Ant 3: 15×80 mmc²

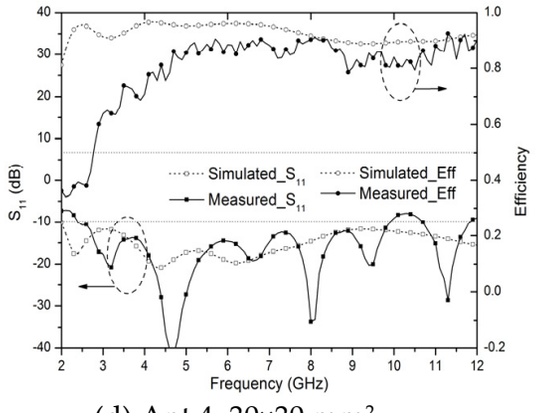


(d) Ant 4: 30×30 mm²

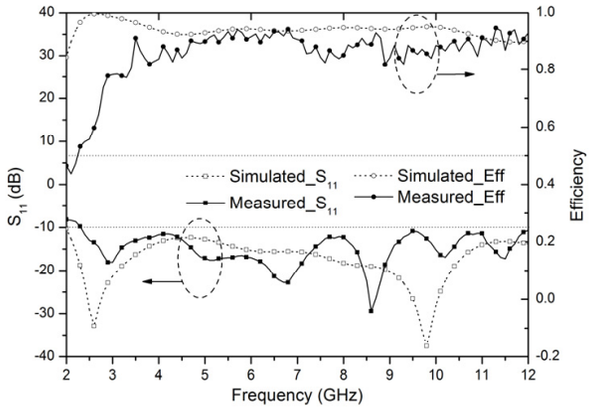


(e) Ant 5: 30×50 mm$^2$

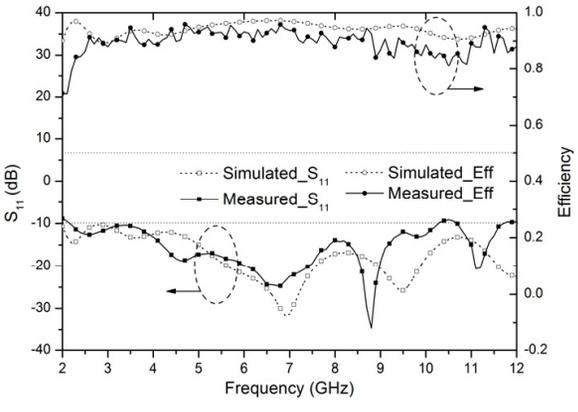


(f) Ant 6: 30×80 mm$^2$

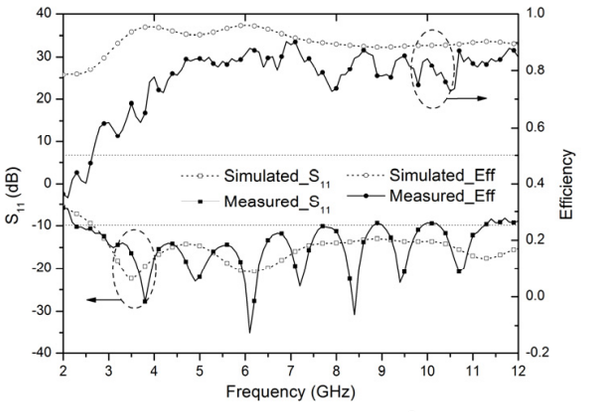


(g) Ant 7: 50×30 mm$^2$

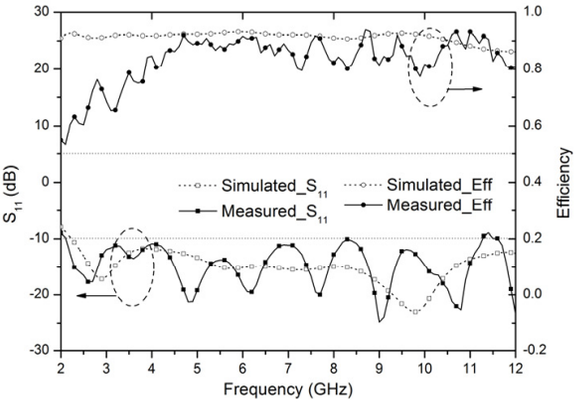


(h) Ant 8: 50×50 mm$^2$

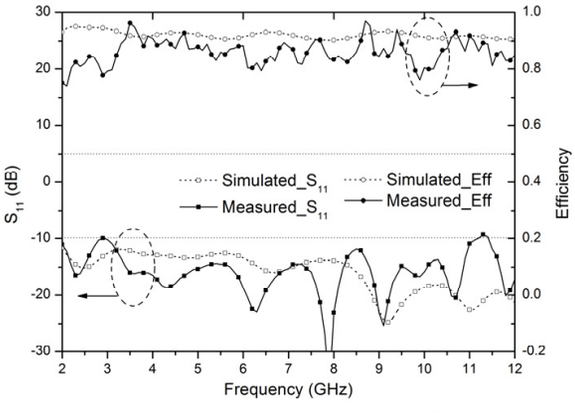


(i) Ant 9: 50×80 mm$^2$

**Figure 9.** Simulated and measured $S_{11}$ and efficiencies of nine antennas with different ground-plane sizes *gl*×*gw*

| **(Ant) GP dimension** | **(1) 15 (*gl*) × 30 (*gw*)=450** | | | **(2) 15 (*gl*) × 50 (*gw*)=750** | | | **(3) 15 (*gl*) × 80 (*gw*)=1200** | | |
|---|---|---|---|---|---|---|---|---|---|
| **Avg. 2-12 GHz** | 0.110 | | | 0.074 | | | 0.040 | | |
| **2-4 GHz, 4-6GHz, 6-12 GHz** | 0.244 | 0.121 | 0.060 | 0.172 | 0.026 | 0.055 | 0.050 | 0.051 | 0.034 |
| **(Ant) GP dimension** | **(4) 30 (*gl*) × 30 (*gw*)=900** | | | **(5) 30 (*gl*) × 50 (*gw*)=1500** | | | **(6) 30 (*gl*) × 80 (*gw*)=2400** | | |
| **Avg. 2-12 GHz** | 0.102 | | | 0.081 | | | 0.049 | | |
| **2-4 GHz, 4-6GHz, 6-12 GHz** | 0.225 | 0.114 | 0.055 | 0.180 | 0.056 | 0.054 | 0.050 | 0.052 | 0.038 |
| **(Ant) GP dimension** | **(7) 50 (*gl*) × 30 (*gw*)=1500** | | | **(8) 50 (*gl*) × 50 (*gw*)=2500** | | | **(9) 50 (*gl*) × 80 (*gw*)=4000** | | |
| **Avg. 2-12 GHz** | 0.151 | | | 0.072 | | | 0.061 | | |
| **2-4 GHz, 4-6GHz, 6-12 GHz** | 0.186 | 0.116 | 0.058 | 0.130 | 0.057 | 0.056 | 0.069 | 0.058 | 0.061 |

**Table 2.** Average discrepancy of efficiency between simulated and measured results (GP: Ground plane)

## 4. Effects of feeding cable on small UWB monopoles measurements

As explained before, the feeding cable used in measurements will scatter, reflect and radiate EM fields, causing interference to the measured results of antennas. Here the effects of the feeding cable are investigated by using simulation and measurement. In the antenna measurement system, Starlab, the feeding cable is enclosed by an EMI suppressant material which is highly lossy. The EM fields incident on it and radiated from it will be absorbed. This significantly reduces unwanted interference to the measured radiation patterns. However, absorbing the EM radiation leads to reduced efficiency. That is why the measured radiation efficiencies are always lower than the simulated results.

### 4.1. Modeling of feeding cables

Here, we describe the simulation models for two types of feeding cables, denoted here as cables A and B as shown in Figures 10(a) and (b), respectively [20], and use the models in our simulation to study their effects on the measurements of the antenna performances. Cable A is just an ordinary coaxial cable, having a center conductor with a radius of 0.45 mm, and an outer conductor with inner and outer radii of 1.5 and 1.8 mm, respectively. Both cables have a length of about 250 mm. Figure 11(a) shows the cross section of cable A. The space between the center and outer conductors is filled with a dielectric Teflon having a permittivity of 2.08. For cable B shown in Figure 10(b), it is a coaxial cable provided by Satimo for use with the antenna measurement system, Starlab. The cross section of the cable is shown in Figure 11(b) which is identical to cable A, except that the cable has an EMI suppressant tube with a thickness of 1.25 mm on the surface. The property of the tubing material is quite complicated and hard to express precisely. Simulation results show that, by setting both the permittivity and the permeability to 5, and the electric and magnetic loss tangents to 0.004 and 0.5, respectively, the discrepancies between the simulated and measured $S_{11}$ and efficiency are much reduced, thus these parameters are used in our simulation model for cable B.

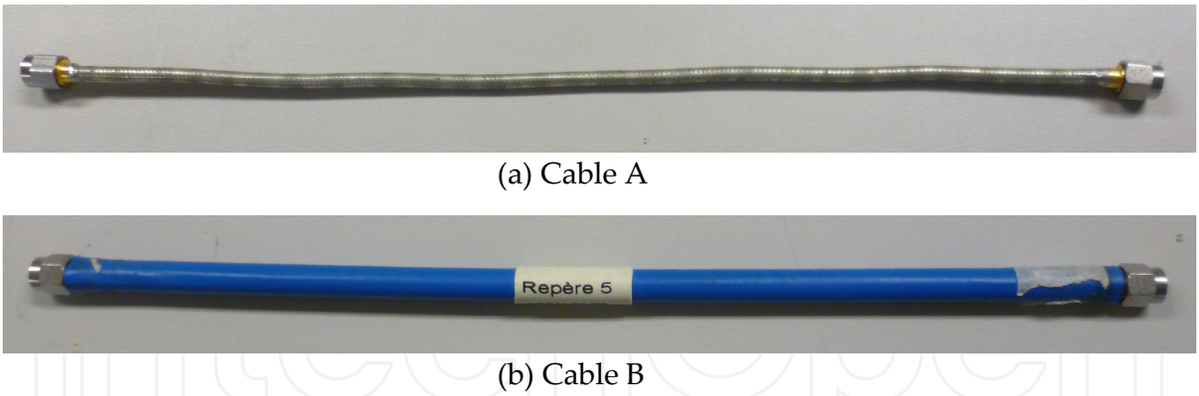


(a) Cable A

(b) Cable B

**Figure 10.** Two types of feeding cables used for studies.

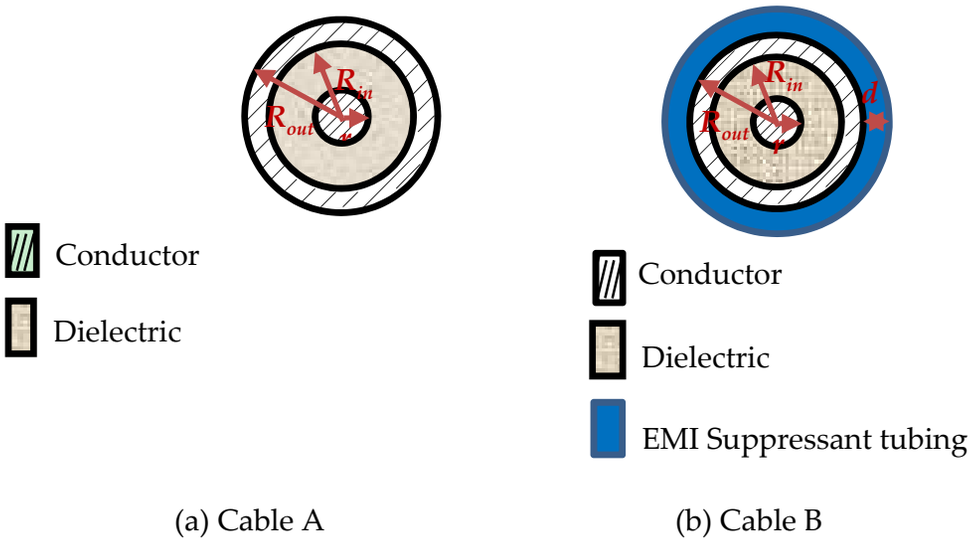


(a) Cable A (b) Cable B

**Figure 11.** Cross sections of cables used for studies

## 4.2. Antennas used for studies

Three of the nine UWB antennas, Ants 4, 5 and 9 with ground-plane sizes ($gl \times gw$ ) of 30 × 30 mm², 30 × 50 mm², and 50 × 80 mm², respectively, shown in Figure 7 are selected for investigation of the cable effects using computer simulation. The simulated models developed for cables A and B are used in simulation to feed the signal to the antenna as shown in Figures 12(a) and (b), respectively. In the Starlab system, there is a system cable with EMI suppressant tubing (similar to that used in cable B) used to connect the feeding cable (cable A or cable B) to the network analyzer of the system. The system cable has a length of about 3-4 m long. However, to reduce the simulation time, we only use a total length of 400 mm in our simulation models. Thus when cable A with a length of 250 mm is used, we append a 150-mm cable B to it, making it a total length of 400 mm, as shown in Fig. 12(a). When cable B with a length of 250 mm is used, we actually use a total length of 400 mm, instead of 250 mm. In Figure 12, a metal brick with a size of 6.5 × 6.5 × 13.5 mm³ is used to model the SMA connector.

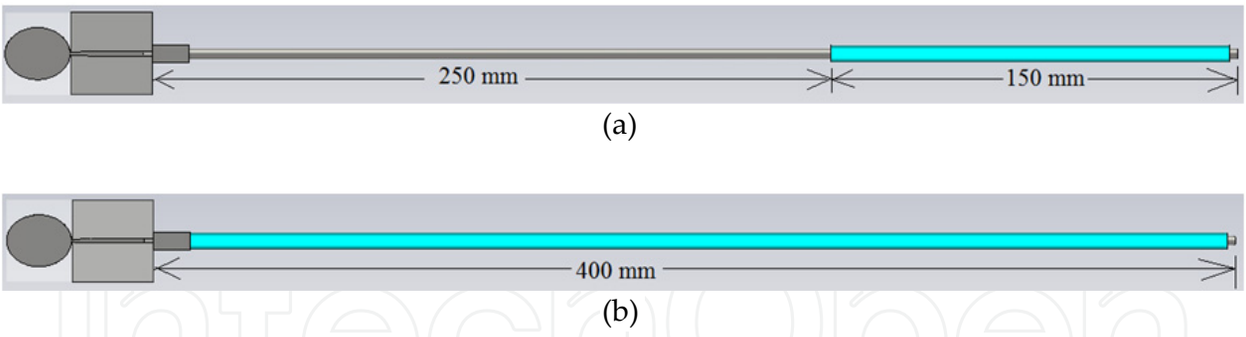


**Figure 12.** Simulation models of antenna connected to (a) cable A, and (b) cable B

## 4.3. Results and discussions

### *4.3.1. Effects of ordinary coaxial cable (cable A)*

With the use of cable A as the feeding cable, the simulated and measured $S_{11}$ and efficiencies of the three antennas are shown in Figure 13. For comparison, the simulation results without a feeding cable are also shown in the same figure. It can be seen in Figure 13 that at high frequencies the simulated efficiencies of the antenna with and without using the cable model are about the same. This is because at high frequencies the ground planes are electrically large, leading to little cable effects on measurements. As the frequency reduces, the ground planes become smaller and discrepancies occur. For impedance bandwidth ($S_{11}$ = -10 dB), all results agree well. This seems to indicate that the cable does not have much effect on the measurements, which as shown later is not true. In fact, at low frequencies, the current flows back from the small ground plane to the surface of the feeding cable, as described previously, giving rise to EM radiation, and then get measured by the system. The measured and simulated results on 3D-radiation patterns reveal that the feeding cable has serious effects on measurements.

The simulated and measured 3D-radiation patterns of the antenna with the ground-plane size of 30 × 30 mm$^2$ at the frequencies of 3, 7 and 11 GHz, are shown in Figure 14. Without using the feeding cable, the simulated result in Figure 14(a) shows that the antenna has an "apple-shape" radiation pattern at the frequency of 3 GHz which is typical for monopole antennas. At higher frequencies of 7 and 11 GHz, the radiation patterns become slightly directional due to operating in the higher modes. However, when cable A is used, the simulated radiation patterns in Figure 14(b) show many ripples, particularly serious at the lower frequency of 3 GHz. This is because, at 3 GHz, the ground-plane size of 30 × 30 mm$^2$ (only about half wavelength) is too small to serve as an infinite ground for the monopole. As showed previously, with a small ground plane, the EM fields radiated from antenna are diffracted at the edges and induce currents to flow back to the feeding cable. This can be seen in Figure 15(a) which shows a snap-shot of the simulated surface-current on the feeding cable at 3 GHz. A standing wave is developed along the feeding cable. This produces secondary EM radiation and causes the ripples on the 3D-radiation patterns of Figure 14(b). At 11 GHz, the ground plane is electrically larger and so the 3D-radiation

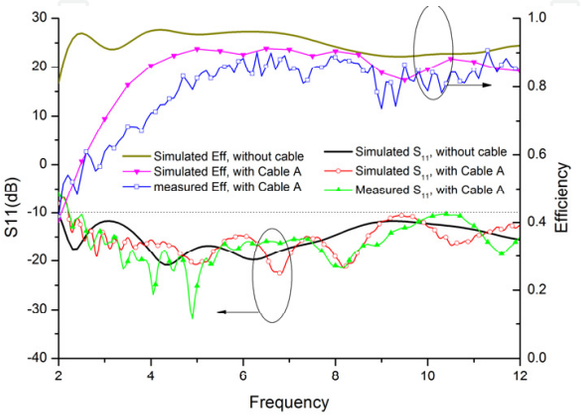


(a) Ant 4: 30 × 30 mm²

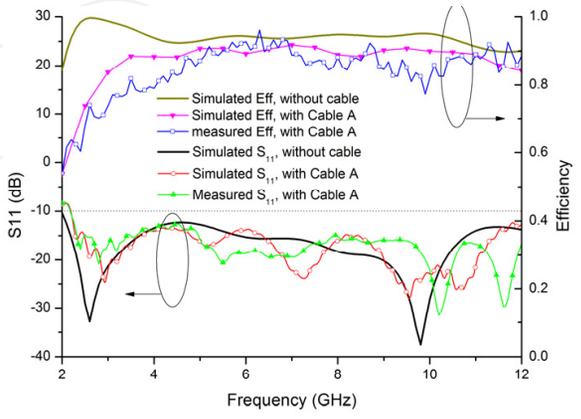


(b) Ant 5: 30 × 50 mm²

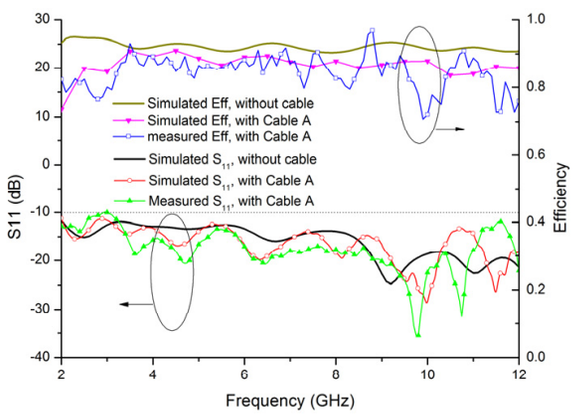


(c) Ant 9: 50 × 80 mm²

**Figure 13.** Simulated and measured S11 and efficiencies using cable A with different ground-plane sizes.

pattern becomes very similar to the corresponding radiation pattern in Figure 14(a) without using the cable. This can also be seen in Figure 15(b) which shows the simulated surface-current on the feeding cable at 11 GHz. The standing wave on the feeding cable becomes insignificant. The measured 3D-radiation patterns using cable A at 3, 7 and 11 GHz are shown in Figure 14(c), indicating very good agreements with the corresponding simulated radiation patterns in Figure 14(a). These results verify the validity of our simulation mode for the cable.

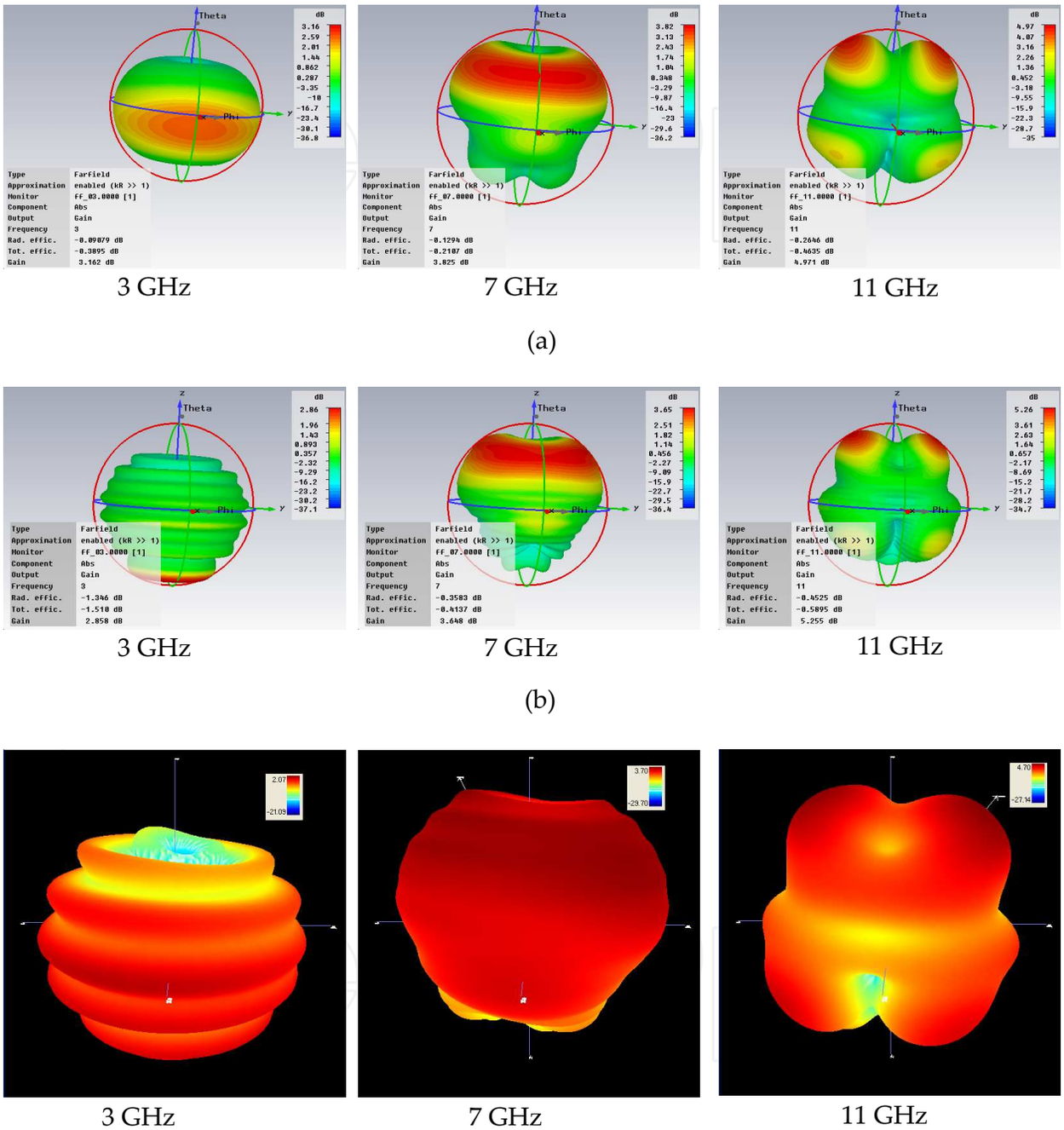


**Figure 14.** 3D-radiation patterns at 3, 7 and 11 GHz. (a) Simulation without cable, (b) simulation using cable A, and (c) measurement using cable A. Ground-plane size: 30 x 30 mm$^2$.

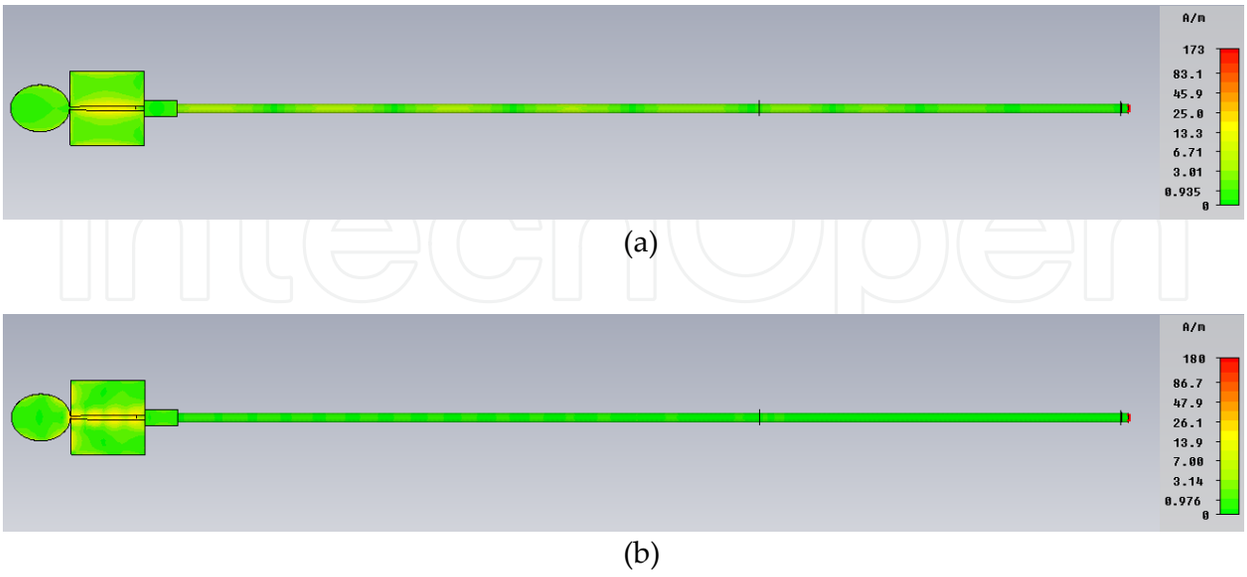


**Figure 15.** Surface current distributions of antenna using cable A at (a) 3 GHz, and (b) 11 GHz

### *4.3.2. Effects of feeding cable with EMI suppressant tubing (cable B)*

Figure 16 shows the simulated and measured results for using cable B. It can be seen that, with the use of the simulation model for cable B, the measured and simulated $S_{11}$ and efficiencies have very good agreements for the three antennas even at lower frequencies. These results confirm the accuracy of our simulation model for the feeding cable used in the antenna measurement system. The simulated results without using the feeding cable are also shown in the same figure for comparison. It can be seen that the simulated efficiency without using the feeding cable at low frequencies is much higher than the simulated or measured efficiencies using the feeding cable. This is because at low frequencies, the current flows back to the feeding cable and causes secondary radiation which is mostly absorbed by the EMI suppressant tube enclosing the cable.

The 3D-radiation patterns of the antenna with a ground-plane size of 30 x 30 $mm^2$ at the frequencies of 3, 7 and 11 GHz are shown in Figure 17. With the use of cable B, Figures 17(b) and (c) show no ripple on the 3D-radiation patterns. The simulated 3D-radiation patterns with and without using cable B agree quite well, indicating the effectiveness of using EMI suppressant tubing for the feeding cable. The measured 3D-radiation patterns in Figure 17(c) are similar to the corresponding simulated radiation patterns shown in Figure 17(b). Figure 18 shows the simulated current distributions on the outer surface of the feeding cable at 3 and 7 GHz. Compared with those in Figure 15, it can be seen that the surface current is very small even at 3 GHz because of the EMI suppressant material. It should be noted that, at low frequencies, since the EM fields radiated from the feeding cable are mostly absorbed by EMI suppressant tubing, the efficiency and hence the gain are much reduced.

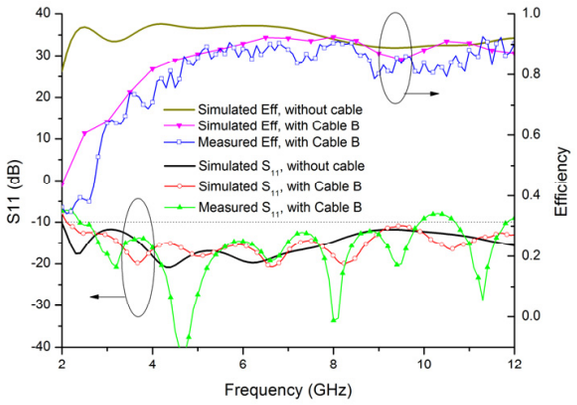


(a) Ant 4: 30 × 30 mm²

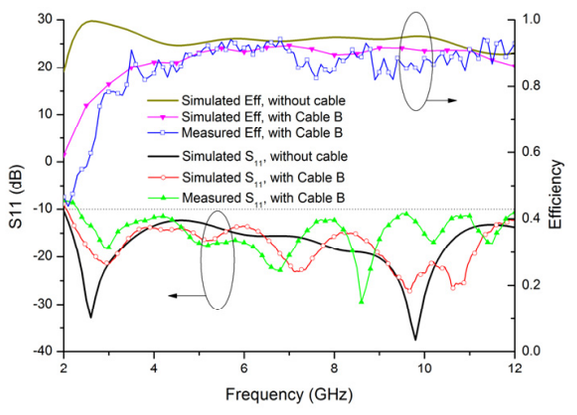


(b) Ant 5: 30 × 50 mm²

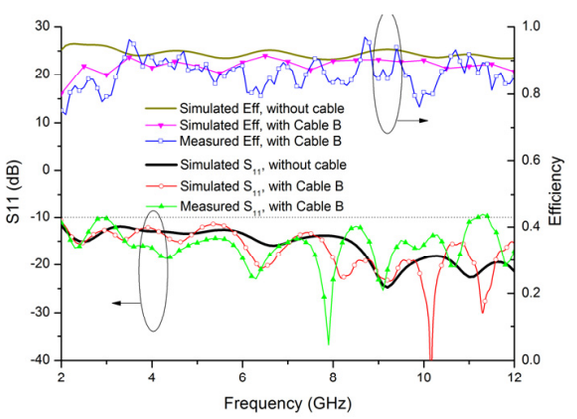


(c) Ant 9: 50 × 80 mm²

**Figure 16.** Simulated and measured $S_{11}$ and efficiencies using cable B with different ground-plane sizes

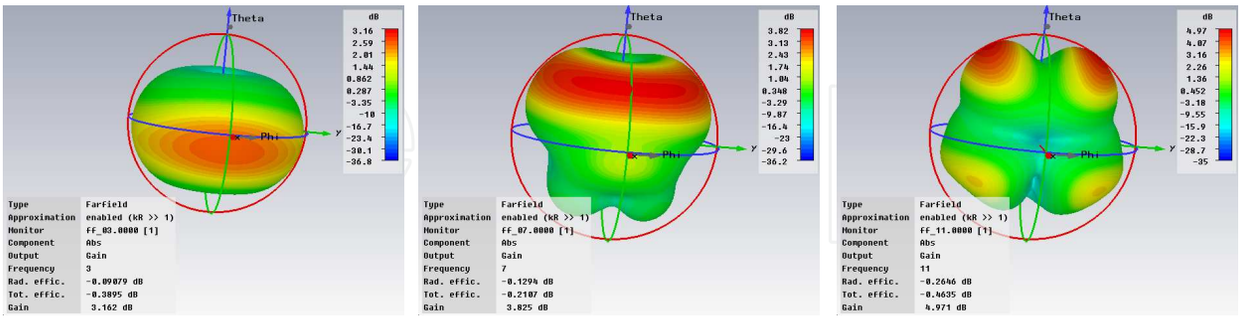


3 GHz 7 GHz 11 GHz

(a)

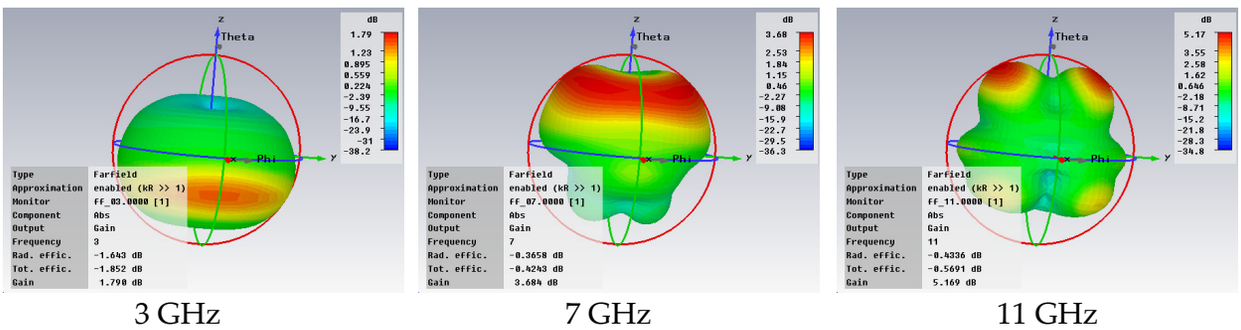


3 GHz 7 GHz 11 GHz

(b)

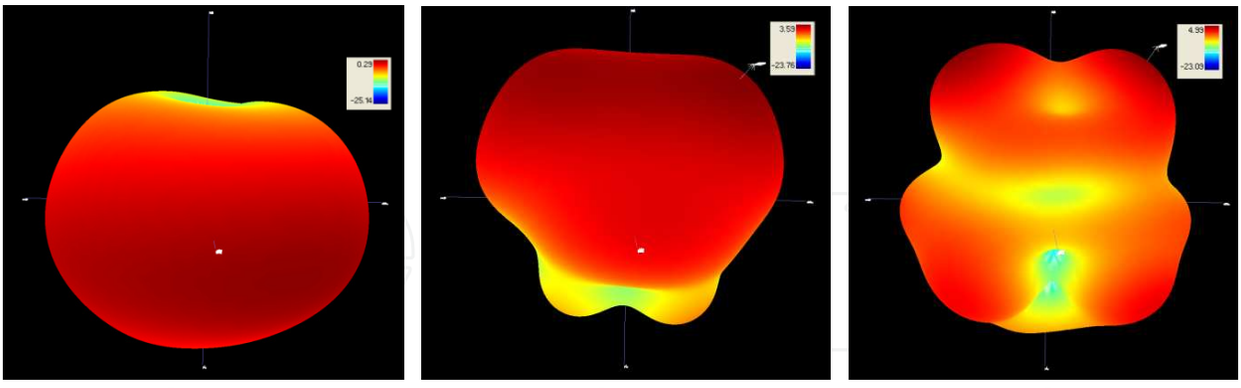

3 GHz 7 GHz 11 GHz

(c)

**Figure 17.** 3D-radiation patterns at 3, 7 and 11 GHz. (a) Simulation without cable, (b) simulation using cable B, and (c) measurement using cable B. Ground-plane size: 30 x 30 mm$^2$.

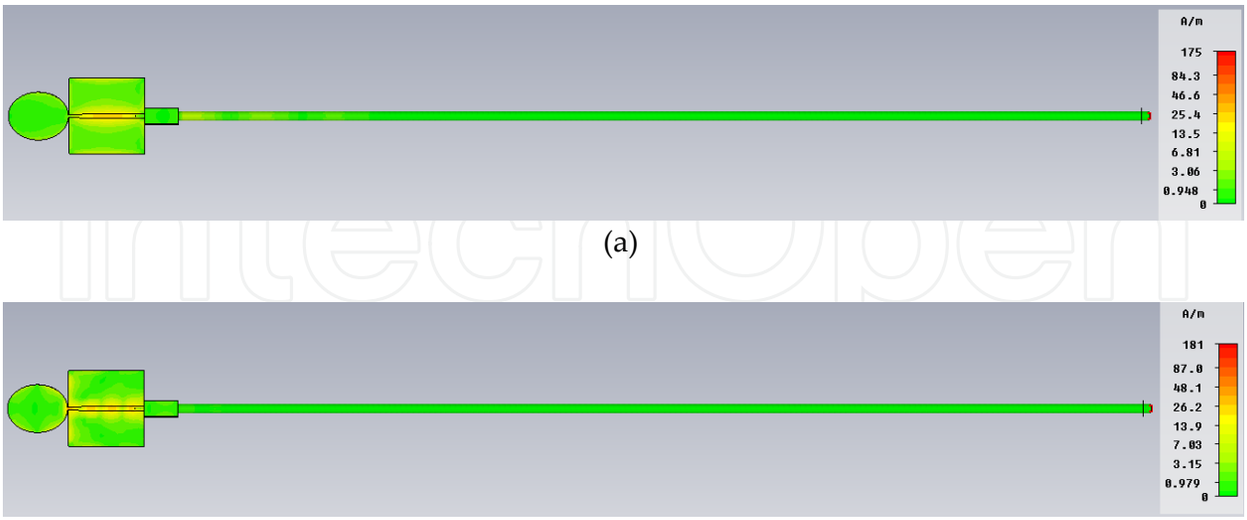


**Figure 18.** Surface current distribution of antenna using cable B at (a) 3 GHz and (b) 11 GHz

## 5. Conclusions

The effects of small ground-plane sizes of planar UWB monopole antennas and feeding cable on measurements have been described and studied using computer simulation and measurement. A group of nine UWB antennas with the same radiator but different ground-plane sizes have been used for studies. Results have shown that the widths of the ground planes have more effects on the measured efficiencies. There are large discrepancies between the simulation and measured performances of these antennas at low frequencies.

The models of two practical feeding cables have been developed for studying the cable effects using computer simulation. Measurement results have verified the accuracies the two simulation models. Both the simulation and measured results have shown the feeding cable without EMI suppressant tubing has significant effects on measurements.

## Author details

L. Liu, S.W. Cheung, Y.F. Weng and T.I. Yuk
*Department of Electrical and Electronic Engineering, The University of Hong Kong, Hong Kong*

## 6. References

[1] Liu L, Cheung SW, TI Yuk (2011) Bandwidth Improvements Using Ground Slots for Compact UWB Microstrip-fed Antennas. Progress In Electromagnetics Research Symposium (PIERS) 2011. Suzhou, China.

[2] Cheung SW, Liu L, Azim R, Islam MT (2011) A Compact Circular-Ring Antenna for Ultra-Wideband Applications. Microwave and Optical Technology Letters. 53: 2283–2288.
[3] Liu L, Cheung SW, Yuk TI (2011) Bandwidth Improvements Using Ground Slots for Compact UWB Microstrip-fed Antennas. Progress In Electromagnetics Research Symposium (PIERS) 2011. Suzhou, China.
[4] Sun YY, Cheung SW, Yuk TI (2011) Studies of Planar Antennas with Different Radiator Shapes for Ultra-wideband Body-centric Wireless Communications. Progress In Electromagnetics Research Symposium (PIERS) 2011. Suzhou, China.
[5] Zhang J, Sun XL, Cheung SW, Yuk TI (2012) CPW-Coupled-Fed Elliptical Monopole Antenna for UWB Applications. IEEE Radio Wireless Week 2012 (RWW2012), Santa Clara, CA, USA
[6] Sun YY, Islam MT, Cheung SW, Yuk TI, Azim T, Misran N (2011) Offset-fed UWB Antenna with Multi-slotted Ground Plane. IEEE International Workshop on Antenna Technology ( iWAT2011), 2011
[7] Sun YY, Cheung SW, Yuk TI (2012) Planar Monopole Ultra-wideband Antennas with Different Radiator Shapes for Body-centric Wireless Networks. Progress In Electromagnetics Research Symposium 2012 (PIERS2012), Kuala Lumpur, Malaysia
[8] Saario SA, Lu JW, Thiel DV (2002) Full-wave analysis of choking characteristics of sleeve balun on coaxial cables. Electronics Letters. 38: 304-305.
[9] Chow YL, Tsang KF, Wong CN (1999) An accurate method to measure the antenna impedance of a portable radio. Microwave and Optical Technology Letters. 23: 349-352.
[10] The Capcon website. Available: http://www.capconemi.com/st4page1.html
[11] The Satimo website. Available: http://www.satimo.com/content/products/starlab
[12] Gandhi OP, Lazzi G, Furse CM. Monopole Antennas. Available: http://www.ece.utah.edu/~ece3300/Labs/lab3/MONOPOLE%20ANTENNAS.pdf
[13] Chen ZN, Chia MYW (2006) Broadband Planar Antennas Design and Applications. West Sussex, England: John Wiley & Sons, Ltd.
[14] Icheln C (2001) Methods for measuring RF radiation properties of small antennas. PhD thesis, Helsinki University of Technology, Espoo, Finland, Nov.
[15] DeMarinis J (1988) The antenna cable as a source of error in EMI measurements. IEEE 1988 International Symposium on Electromagnetic Compatibility Symposium Record. pp 9-14.
[16] Weiner MM, (2003) Monopole Antennas. NY: Marcel Dekker, Inc.
[17] Awadalla K, Maclean T (1979) Monopole antenna at center of circular ground plane: Input impedance and radiation pattern. IEEE Transactions on Antennas and Propagation. 27: 151-153.
[18] Weng YF, Cheung SW, Yuk TI (2010) Effects of ground-plane size on planar UWB monopole antenna. TENCON 2010. pp. 422-425.
[19] Icheln C, Ollikainen J, Vainikainen P (1999) Reducing the influence of feed cables on small antenna measurements. Electronics Letters. 35: 1212-1214.

[20] Liu L, Weng YF, Cheung SW, Yuk TI Foged LJ (2011) Modeling of cable for measurements of small monopole antennas. Loughborough Antennas & Propagation Conference (LAPC) 2011, Loughborough, UK.

IntechOpen

IntechOpen